Thermochimica Acta, 184 (1991) 141–150
Elsevier Science Publishers B.V., Amsterdam

Kinetic analysis of thermal decomposition reactions. Part 5. Gamma irradiation effects on the thermal decomposition of potassium nickel oxalate

El-H.M. Diefallah[1], S.N. Basahl, M.M. El-Fass and E.A. Al-Sabban

Department of Chemistry, Faculty of Science, King Abdulaziz University, Jeddah (Saudi Arabia)

(Received 31 October 1990)

Abstract

Differential thermal analysis–thermogravimetry techniques were used to study the thermal decomposition of potassium nickel(II) oxalate hexahydrate crystals and the effects of ^{60}Co gamma irradiation on the kinetics of the decomposition in air of $K_2Ni(C_2O_4)_2$ to NiO, $K_2C_2O_4$ and CO_2. The kinetics of the isothermal decomposition were studied over the temperature range 310–350 °C, both for irradiated and non-irradiated $K_2Ni(C_2O_4)_2 \cdot 6H_2O$ crystals. Kinetic analysis of the results according to the various theoretical models of solid state reactions showed that the best fit is obtained for the first-order and the diffusion models. There is a decrease in both the energy of activation and the frequency factor with increasing radiation dose. The mechanism of the thermal decomposition and the effects produced by radiolysis were discussed.

INTRODUCTION

The absorption of ionizing radiations by a substance results in a variety of physical and chemical consequences which depend on the nature of the system and the energy of the incident radiation [1–3]. Irradiation seems to create many new potential nucleation centres which favour heterogeneous processes. In general, while the action of irradiation on one chemical compound might be predominantly electronic, the action on another may be mostly structural. Previous studies have also shown that radiation damage in crystalline solids recovers when the irradiated crystals are heated. However, there is little information regarding the relative competition between thermal decomposition and thermal annealing of the damage in irradiated solids.

The kinetics and mechanism of solid state thermal dehydration and decomposition reactions of simple metal salts have attracted the interest of

[1] Author to whom correspondence should be addressed. Present address: Department of Chemistry, Faculty of Science, Benha University, Benha, Egypt.

0040-6031/91/$03.50

several investigators [4]. While there have been relatively few studies on thermoanalytical applications to the chemistry of coordination compounds [5–7], there are even fewer on the kinetics of thermal decomposition reactions of complexes. Danforth and Dix [8] have concluded that the energy barrier to the thermal decomposition of magnesium and zinc oxalates is not diminished by the product oxide and suggested that the reaction rate is controlled by an electron-transfer step. In studying the decomposition of potassium tris(oxalato)ferrate(III) [9], it was concluded that the product, iron(II) oxalate, has an acceleratory effect on the reaction. In the decomposition of nickel oxalate [10], the reaction commences at dislocations and proceeds through the catalytic breakdown of the anion on the product metal surface.

Numerous irradiation effects on simple metal oxalates have been described [1–3] with particular emphasis on the silver [11,12] and nickel [13] compounds. The fractional reaction α vs. time t curves are always sigmoidal and show the exponential and power-law types of dependence. In general, the exponential law is regarded as indicative of the branching of a growing nucleus (i.e. a chain reaction), whereas the power law indicates a fixed topochemical scheme in one, two or three dimensions.

In the present study, we have used thermogravimetry to study the thermal decomposition of potassium nickel oxalate hexahydrate and the effects of ^{60}Co gamma irradiation on the kinetics of the isothermal decomposition reaction.

EXPERIMENTAL

Potassium nickel(II) oxalate hexahydrate was prepared by slowly adding nickel oxalate to a hot saturated solution of potassium oxalate until no more would dissolve [14]. The excess nickel oxalate was filtered off and the filtrate was cooled overnight. The complex crystallised from solution as dark turquoise crystals; it was filtered under suction until dry and kept in a desiccator. The product was sieved to obtain crystals less than 125 μm in diameter for irradiation.

Samples (10 mg) were placed in clean glass-stoppered Pyrex tubes and irradiated in air in a ^{60}Co-Gammacell 220 (Atomic Energy of Canada, Ltd., Commercial Products Div., Ottawa, Canada). Samples were exposed to successively increasing doses of radiation at constant intensity. The source was calibrated against a Fricke ferrous sulphate dosimeter [15] and the dose rate in the irradiated samples was calculated by applying appropriate corrections on the basis of the average mass–energy absorption coefficient for the sample and the dosimeter solution.

The thermal behaviour of irradiated and non-irradiated $K_2Ni(C_2O_4)_2 \cdot 6H_2O$ crystals was investigated using a Shimadzu Model 30 thermal analyser. Differential thermal analysis–thermogravimetry (DTA–TG) curves were

recorded in an atmosphere of nitrogen (flow rate, 50 ml min^{-1}) and in air (flow rate, 30 ml min^{-1}). The kinetics of the second stage of the thermal decomposition of $K_2Ni(C_2O_4)_2 \cdot 6H_2O$ was followed in the temperature range 310–350 °C. In order to ensure a linear heating rate and accurate temperature measurements, the sample weights in the platinum cell of the thermal analyser were about 6–8 mg.

RESULTS AND DISCUSSION

The DTA–TG studies showed that the thermal decomposition of $K_2Ni(C_2O_4)_2 \cdot 6H_2O$ at temperatures below 800 °C occurs in two steps [14]. Typical DTA–TG curves in N_2 and air atmospheres are shown in Figs. 1 and 2 respectively. The DTA peaks closely correspond to the weight changes observed on the TG curve. In nitrogen, the first step starts at about 35 °C; it

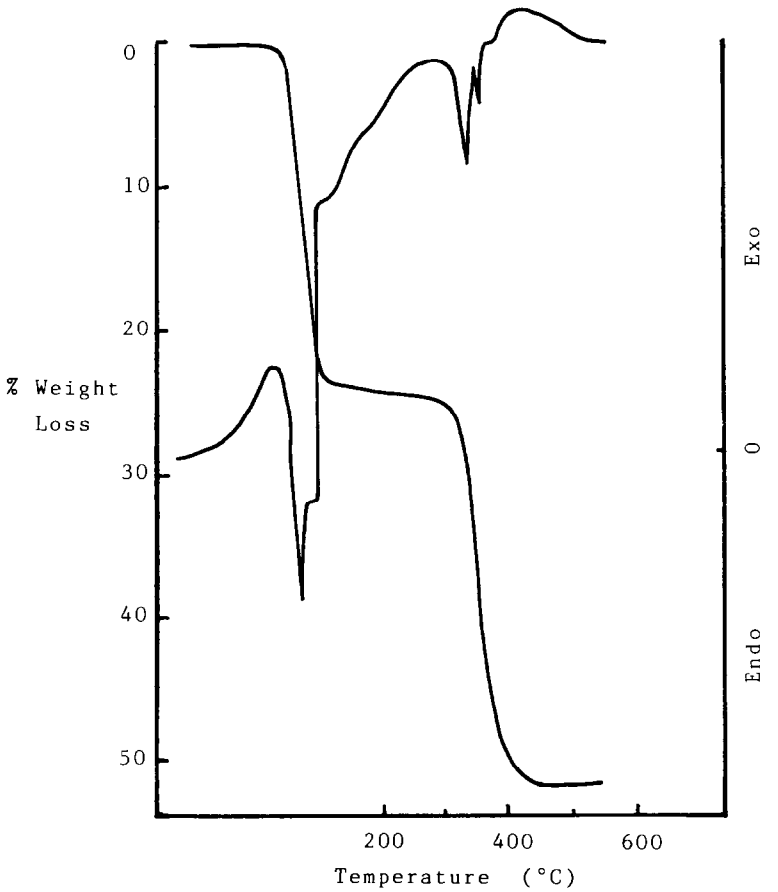

Fig. 1. DTA–TG curves of $K_2Ni(C_2O_4)_2 \cdot 6H_2O$ in nitrogen.

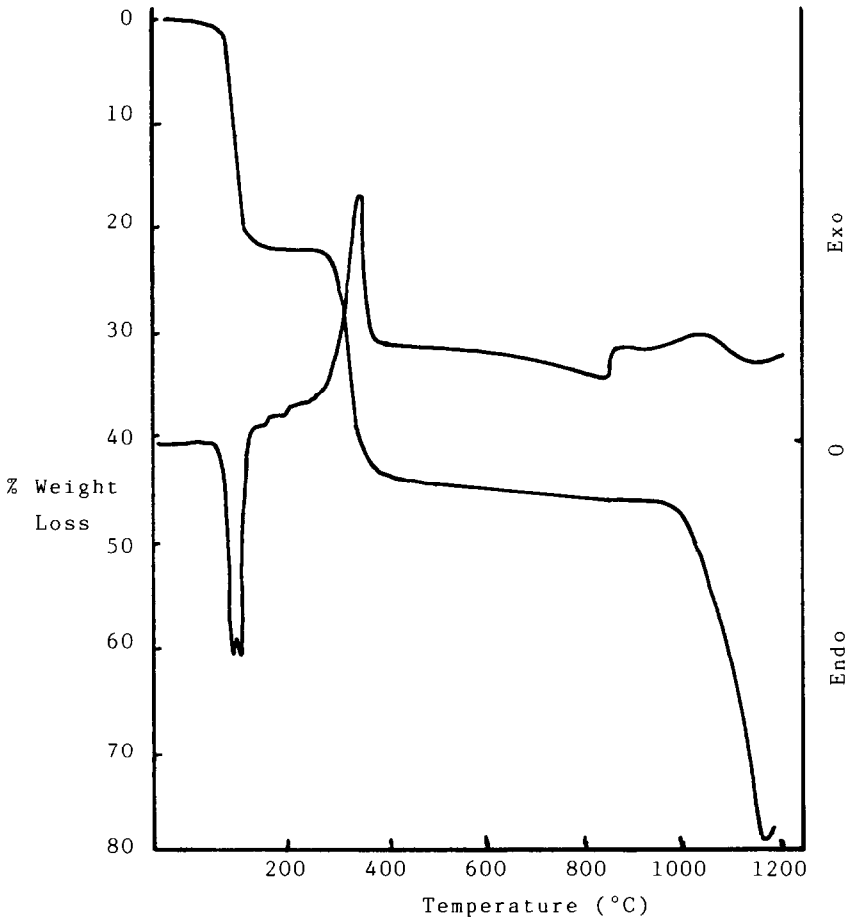

Fig. 2. DTA–TG curves of $K_2Ni(C_2O_4)_2 \cdot 6H_2O$ in air.

is characterised by a broad endothermic peak at 65 °C and indicates a weight loss of 25.7%, attributable to the loss of water of crystallisation. The DTA curve of this step shows a number of small peaks with four minima in the range 50–120 °C, indicating that the loss of the six water molecules proceeds in about four stages. Dehydration is complete at about 110 °C and the anhydrous salt is stable up to about 300 °C. The second decomposition step is also endothermic and indicates a weight loss of 53.2% which is complete at about 485 °C; this is due to the decomposition of the anhydrous salt to potassium carbonate and nickel. This step is characterised by two small endothermic peaks at about 290 and 310 °C which indicate that the decomposition consists of at least two stages.

The thermal decomposition in air (Fig. 2) shows a broad endothermic peak in the range 40–100 °C owing to loss of the water of crystallisation.

The dehydration is complete at 110 °C, showing that all the six H_2O molecules are lattice water: coordinated water molecules are usually eliminated at higher temperatures [16]. In addition, a second step starts at 300 °C, indicating a weight loss of 49.3% which is complete at 470 °C, this is due to the decomposition of $K_2Ni(C_2O_4)_2$ to K_2CO_3 and NiO. This peak is interrupted by an exothermic peak at 325 °C, probably due to air oxidation of CO to CO_2. Above 800 °C, the thermal decomposition residue is K_2O and NiO in air or K_2O and nickel in nitrogen. Broadbent et al. [14] showed that X-ray powder diffraction photographs of samples heated up to 1000 °C still indicate the presence of potassium carbonate in addition to the metal or its oxide.

The two-step mechanism of decomposition of the anhydrous complex could involve the rupture of two Ni–O bonds, the liberation of one CO molecule and the intermediate formation of NiC_2O_4, followed by decomposition of the latter, in the second step, to the oxide in air or the metal in nitrogen. Decomposition will occur when a temperature is reached at which rupture of the M–O bond is possible or at which rupture of the C–O bond occurs. Kahwa and Mulokozi [17] studied the C–C bond distance in metal oxalates, $M\langle^{O_I-C=O_{II}}_{O_I-C=O_{II}}$, and the activation energy and onset temperature of oxalate decomposition, and concluded that the thermolysis mechanism of ionic metal oxalates involves the initial rupture of the $C-O_I$ bonds. Fujita et al. [18] suggested from IR spectral studies that as the $M-O_I$ bond becomes stronger, so the $C-O_I$ bond is lengthened and the $C-O_{II}$ bond is shortened. If the reaction proceeds by rupture of the $C-O_I$ bond, this would be followed by rupture of the $M-O_I$ bond because of the inability of the metal to accommodate two oxygen atoms. In nitrogen, the decomposition temperature represents the temperature at which the $M-O_I$ link is ruptured and this depends critically on the size and charge of the metal ion [19].

The kinetics of the isothermal reaction for the decomposition of the nickel oxalate complex (second stage in $K_2Ni(C_2O_4)_2 \cdot 6H_2O$ decomposition) have been studied for the non-irradiated and the gamma-irradiated crystals. Figure 3 shows typical plots of the fraction decomposed (α) vs. time for the non-irradiated samples. The α–t data were analysed by linear regression (LR) analysis according to the various theoretical models [20–23] listed in Table 1, where $g(\alpha) = kt$. The results of the kinetic analysis showed that the best fit of the data, of both the non-irradiated and irradiated $K_2Ni(C_2O_4)_2 \cdot 6H_2O$ crystals, is obtained according to the F_1 and diffusion models (D_2, D_3 and D_4 equations); the random nucleation models (A_2 and A_3 equations) gave less satisfactory fits. However, irradiation tends to shift the reaction mechanism more towards the diffusion models.

The reduced-time theoretical method [24] was used to choose between the F_1 and the diffusion models. Reduced-time plots have been used by several investigators to decide on the model describing the reaction interface. In this method, master curves showing the variation of α with $t/t_{1/2}$ were calcu-

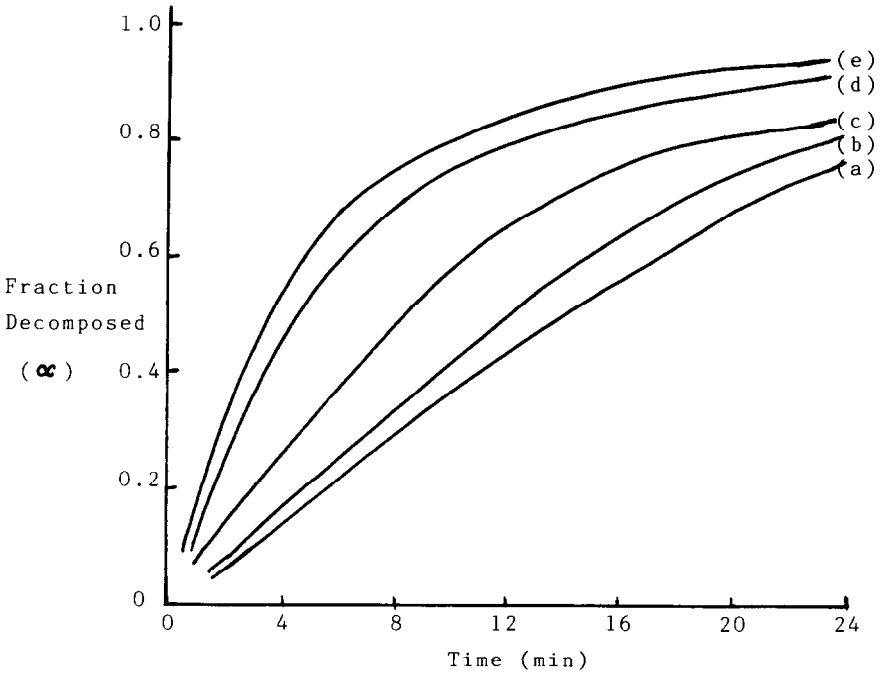

Fig. 3. Isothermal $\alpha-t$ curves for second-stage decomposition of non-irradiated $K_2Ni(C_2O_4)_2 \cdot 6H_2O$: curve (a) 548.5; curve (b) 593; curve (c) 603.5; curve (d) 610.5; and curve (e) 618.5 °C.

lated by Sharp et al. [22] for the different kinetic models. The time scale in the kinetic equations, $g(\alpha) = kt$, is altered so that $g(\alpha) = A(t/t_{1/2})$, where $t_{1/2}$ is the time for 50% reaction and A is a calculable constant depending on the form of $g(\alpha)$. When F_1, D_2, D_3 and D_4 functions are treated in this

TABLE 1

Kinetic equations examined in this work

Reaction model	$g(\alpha)$	Function symbol
One-dimensional diffusion	α^2	D_1
Two-dimensional diffusion	$\alpha + (1-\alpha)\ln(1-\alpha)$	D_2
Jander equation, three-dimensional diffusion	$[1-(1-\alpha)^{1/3}]^2$	D_3
Ginstling–Brounshtein equation, three-dimensional diffusion	$(1-2\alpha/3)-(1-\alpha)^{2/3}$	D_4
Two-dimensional phase boundary reaction	$[1-(1-\alpha)^{1/2}]$	R_2
Three-dimensional phase boundary reaction	$[1-(1-\alpha)^{1/3}]$	R_3
First-order kinetics	$[-\ln(1-\alpha)$	F_1
Random nucleation: Avrami equation	$[-\ln(1-\alpha)]^{1/2}$	A_2
Random nucleation: Erofeev equation	$[-\ln(1-\alpha)]^{1/3}$	A_3

way the following expressions are obtained:

$$F_1(\alpha) = -\ln(1-\alpha) = 0.693(t/t_{1/2}) \quad (1)$$

$$D_2(\alpha) = (1-\alpha)\ln(1-\alpha) + \alpha = 0.1534(t/t_{1/2}) \quad (2)$$

$$D_3(\alpha) = \left(1-(1-\alpha)^{1/3}\right)^2 = 0.0426(t/t_{1/2}) \quad (3)$$

$$D_4(\alpha) = (1-2\alpha/3) - (1-\alpha)^{2/3} = 0.0367(t/t_{1/2}) \quad (4)$$

Hence $t/t_{1/2}$ may be calculated for different values of α and plotted vs. α to get master theoretical curves. To compare experimental data with the master data, the time $t_{1/2}$ corresponding to $\alpha = 0.5$ is determined and the data are converted to curves of α against $t/t_{1/2}$. Figure 4 shows that the experimental data give the best superposition to the master curve of the F_1 model in the acceleratory and fast stages. In the decay stage, the experimental data tend more towards the diffusion models.

In general, there is no simple model which gives a complete fit of the experimental results over the whole fractional reaction range. Analysis of data over α values ranging between 0.10 and 0.80 showed that the F_1 and diffusion models give better fits with higher correlation coefficients than if the α values were taken over the whole fractional reaction range. The rate constants obtained according to these models were used to calculate the

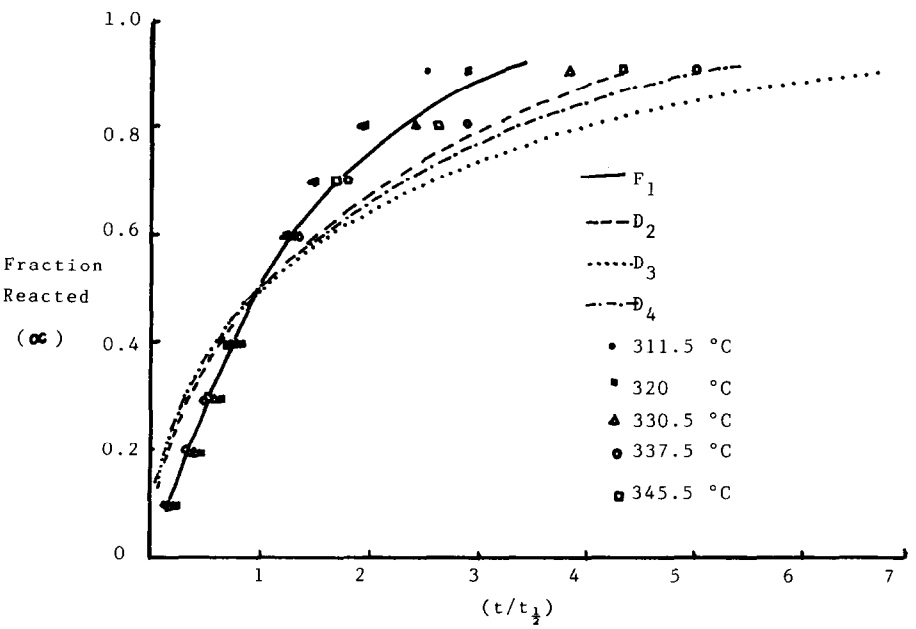

Fig. 4. Reduced plots for the isothermal decomposition of non-irradiated potassium nickel (II) oxalate using F_1, D_2, D_3 and D_4 models.

TABLE 2

Effect of gamma irradiation on the kinetic parameters of the second-stage isothermal decomposition of $K_2Ni(C_2O_4)_2 \cdot 6H_2O$

Dose (MGy)	F_1 function		D_2 function		D_3 function		D_4 function	
	E (kJ mol^{-1})	ln A (min^{-1})	E (kJ mol^{-1})	ln A (min^{-1})	E (kJ mol^{-1})	ln A (min^{-1})	E (kJ mol^{-1})	ln A (min^{-1})
Non-irradiated	77.8	13.2	83.4	13.2	82.8	12.1	80.7	11.3
0.23	75.0	12.6	78.2	12.1	81.3	11.8	79.3	11.0
0.71	73.3	12.1	73.7	11.0	76.0	10.5	74.5	9.9
1.18	52.3	8.1	52.6	7.0	47.7	5.1	52.3	5.6

activation parameters of the reaction as a function of dose, according to the Arrhenius equation, using LR analysis. The results given in Table 2 show that both the energy of activation and the frequency factor decrease with increasing radiation dose. Radiation effects on activation parameters have generally been discussed from the point of view of the catalytic effects of the radiolysis products or of the effects produced on the diffusion process in the solid [20]. In the thermal decomposition of $K_2Ni(C_2O_4)_2 \cdot 6H_2O$, the evolution of the water molecules during the first-stage dehydration step would lower the activation energy of the second-stage thermal decomposition reaction by introducing vacancies and increasing the number of nucleation centres. Moreover, in the thermal decomposition of the irradiated samples, radiation seems to further increase the number of nucleation centres and the porosity of the crystals rather than compensate for radiation annealing of vacancies and nucleation centres.

REFERENCES

1 J. Jach, The Thermal Decomposition of Irradiated Materials, in G.J. Dienes (Ed.), Studies in Radiation Effects on Solids, Vol. 2, Gordon and Breach, New York, 1967, p. 151.
2 D.S. Billington and H.J. Crawford, Jr., Radiation Damage in Solids, Princeton University Press, Princeton, NJ, 1961.
3 V.V. Boldyrev, M. Bulens and B. Delman, The Control of the Reactivity of Solids, Elsevier, Amsterdam, 1979.
4 A.K. Galwey, in MTP International Review of Science, Inorganic Chemistry, Series Two, Solid State Chemistry, Vol. 10, H.J. Emelius (Ed.), Butterworths, London, 1975, p. 147.
5 P.K. Gallagher, in H. Kambe and P.D. Garn (Eds.), Thermal Analysis, Wiley, New York, 1974, p. 17.
6 W.W. Wendlandt and J.P. Smith, The Thermal Properties of Transition Metal Ammine Complexes, Elsevier, Amsterdam, 1976.
7 D. Broadbent, D. Dollimore and J. Dollimore, J. Chem. Soc. A, (1967) 451.
8 J.D. Danforth and J. Dix, J. Am. Chem. Soc., 93 (1971) 6843.
9 J.D. Danforth and J. Dix, Inorg. Chem., 10 (1971) 1623.
10 L. Tournayan, H. Charcosset, B.R. Wheeler, J.M. McGinn and A.K. Galwey, J. Chem. Soc. A, (1971) 868.
11 H. Jost, J. Jedamzik, U. Proesch and I. Ebert, Z. Chem., 25 (1985) 191.
12 R.M. Haynes and D.A. Young, Discuss. Faraday Soc., 31 (1961) 229.
13 J. Jach and M. Griffel, J. Phys. Chem., 68 (1964) 731.
14 D. Broadbent, D. Dollimore and J. Dollimore, in R.F. Schwenker, Jr., and P.D. Garn (Eds.), Thermal Analysis, Vol. II, Academic Press, New York, 1969, p. 739.
15 J.W. Spinks and R.J. Woods, An Introduction to Radiation Chemistry, 2nd edn., Wiley, New York, 1975.
16 A.V. Nikolaev, V.A. Lagvinenko and L.I. Myachina, in R.F. Schenker, Jr., and P.D. Garn (Eds.), Thermal Analysis, Vol. II, Academic Press, New York, 1969, p. 779.
17 I.A. Kahwa and A.M. Mulokozi, J. Therm. Anal., 24 (1982) 265.
18 J. Fujita, K. Nakamoto and M. Kabayashi, J. Phys. Chem., 61 (1957) 1014.
19 D. Dollimore, D.L. Griffiths and D. Nicholson, J. Chem. Soc., (1963) 2617.

20 W.W. Wendlandt, Thermal Methods of Analysis, Wiley-Interscience, New York, 1964.
21 S.F. Hulbert and J.J. Klawitter, J. Am. Ceram. Soc., 50 (1967) 484.
22 J.H. Sharp, G.W. Bindley and B.N.N. Achar, J. Am. Ceram. Soc., 49 (1966) 379.
23 M.E. Brown, Introduction to Thermal Analysis, Chapman and Hall, New York, 1988, Chapter 13.
24 L.F. Jones, D. Dollimore and T. Nicklin, Thermochim. Acta, 13 (1977) 240.